

**Supporting Information For:**

# Synthesis and Characterization of Tunable, pH-Responsive Nanoparticle-Microgel Composites for Surface-Enhanced Raman Scattering (SERS) Detection

Tyler Curtis<sup>†</sup>, Audrey K. Taylor<sup>†</sup>, Sasha E. Alden<sup>†</sup>, Christopher Swanson<sup>†</sup>, Joelle Lo<sup>†</sup>, Liam Knight<sup>†</sup>, Alyson Silva<sup>†</sup>, Byron D. Gates,<sup>¶</sup> Steven R. Emory<sup>†</sup> and David A. Rider<sup>†,‡\*</sup>

<sup>†</sup> - Chemistry Department, Western Washington University, 516 High Street, Bellingham Washington, USA, 98225

<sup>‡</sup> - Department of Engineering and Design, Western Washington University, 516 High Street, Bellingham Washington, USA, 98225

<sup>¶</sup> - Department of Chemistry, Simon Fraser University, 8888 University Drive, Burnaby, Canada, V5A 1S6

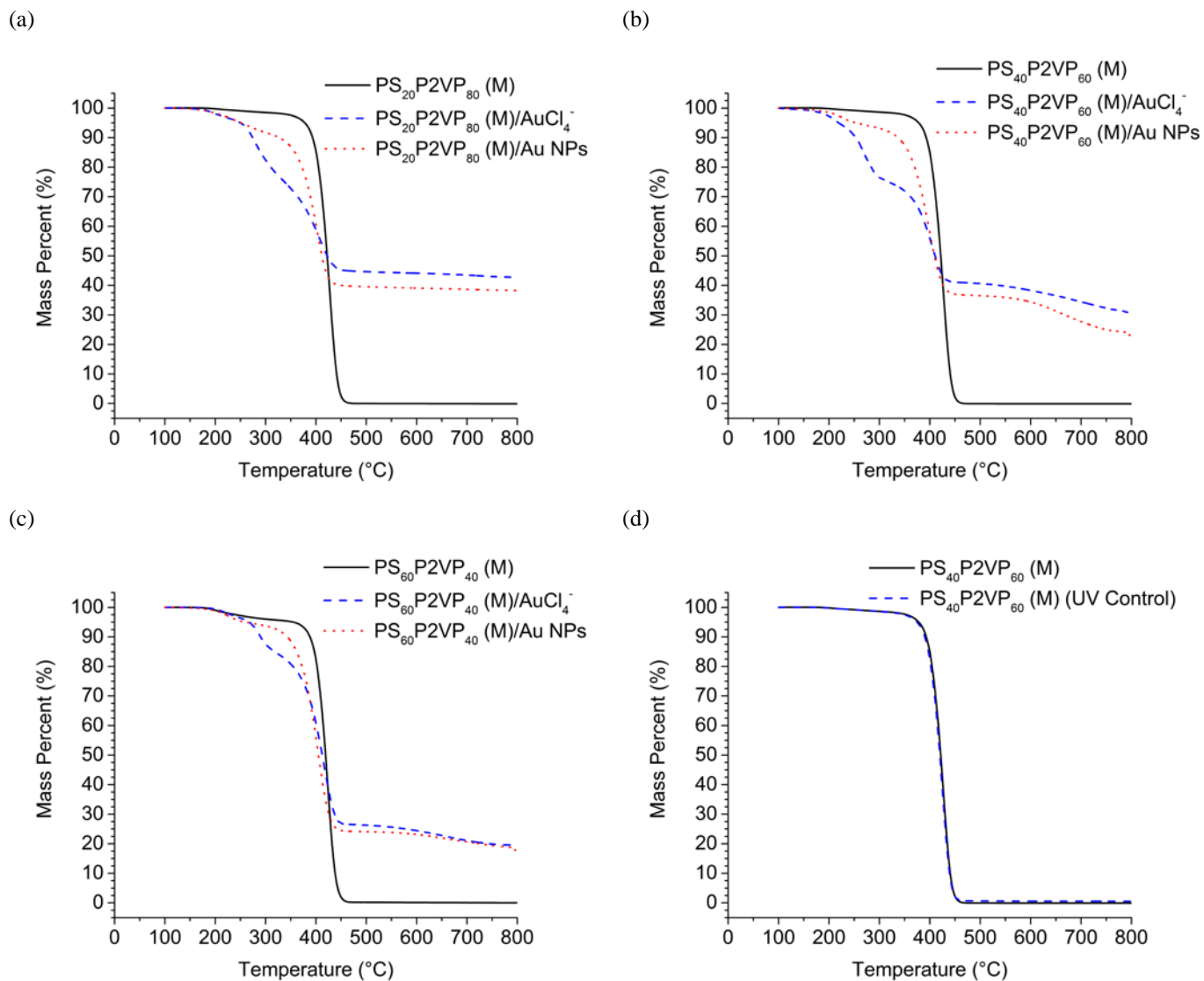


**Figure S1.** TGA curves for (a) PS<sub>20</sub>P2VP<sub>80</sub> (M), PS<sub>20</sub>P2VP<sub>80</sub> (M)/AuCl<sub>4</sub><sup>-</sup>, PS<sub>20</sub>P2VP<sub>80</sub> (M)/Au NPs, (b) PS<sub>40</sub>P2VP<sub>60</sub> (M), PS<sub>40</sub>P2VP<sub>60</sub> (M)/AuCl<sub>4</sub><sup>-</sup>, PS<sub>40</sub>P2VP<sub>60</sub> (M)/Au NPs, (c) PS<sub>60</sub>P2VP<sub>40</sub> (M), PS<sub>60</sub>P2VP<sub>40</sub> (M)/AuCl<sub>4</sub><sup>-</sup>, PS<sub>60</sub>P2VP<sub>40</sub> (M)/Au NPs, (d) PS<sub>40</sub>P2VP<sub>60</sub> (M), and a sample of PS<sub>40</sub>P2VP<sub>60</sub> (M) treated to the UV photoreduction condition.

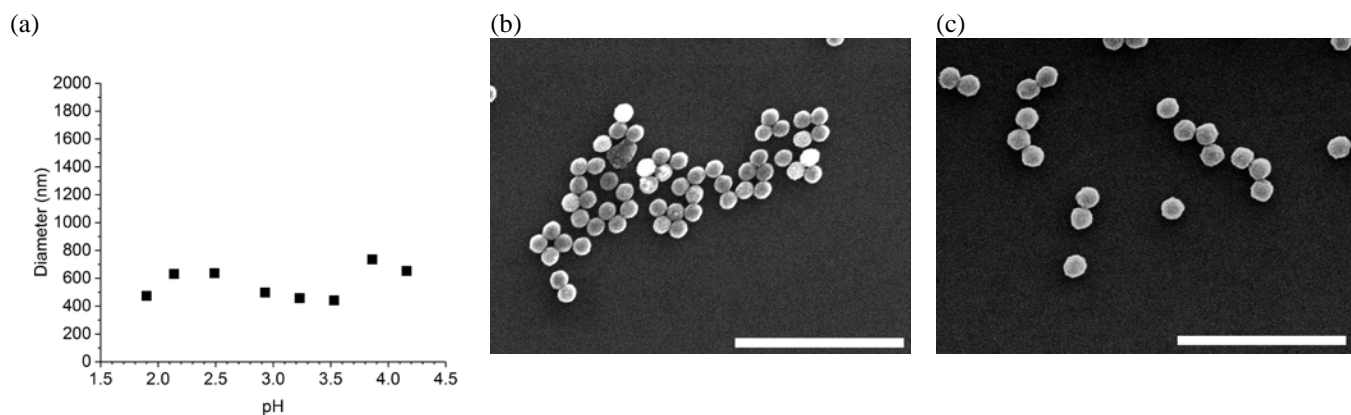


**Figure S2.** (a) Titration curve relating  $D_H$  (by DLS) to pH for PS<sub>20</sub>P2VP<sub>80</sub> (M)/Au NPs. SEM images of (b) PS<sub>40</sub>P2VP<sub>60</sub> (M)/Au NPs and (c) PS<sub>60</sub>P2VP<sub>40</sub> (M)/Au NPs. Scale bar = 2 μm.

**Movie S1.** Video depicting the 3-dimensional reconstruction of a PS<sub>0</sub>P2VP<sub>100</sub> (M)/Au NPs composite that was prepared from photoreduced PS<sub>0</sub>P2VP<sub>100</sub> (M)/AuCl<sub>4</sub><sup>-</sup> (generated by loading with KAuCl<sub>4</sub> using a pH = 1, H<sub>2</sub>SO<sub>4</sub> solution). A series of TEM images were acquired by tilting the TEM grid from -70° to +70° with 2° increments. The Inspect3D software used a contrast thresholding condition to identify Au NPs. These NPs are shown with red pixels in the later portion of the video and Figure S3. The magnification is 320,000x.

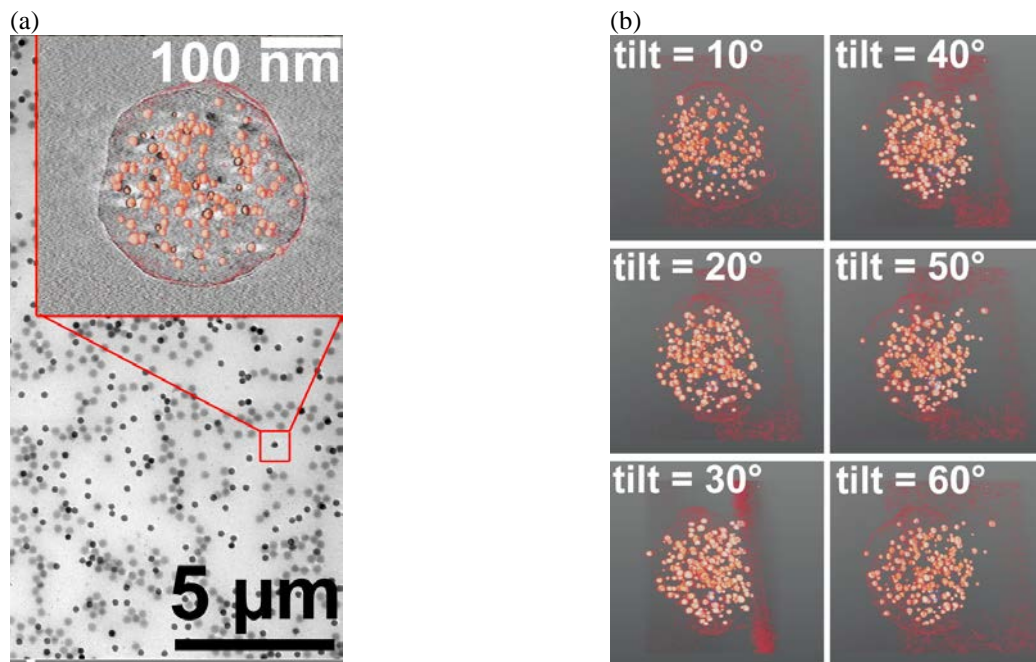
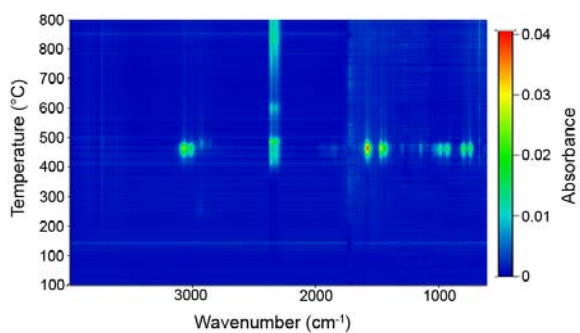
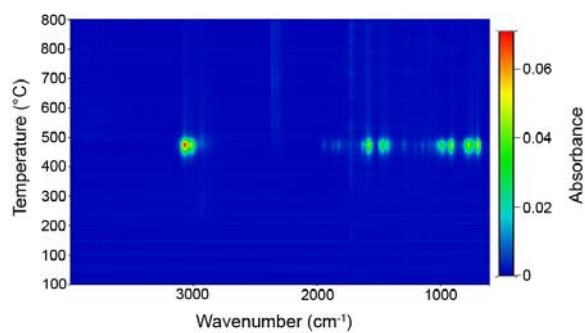


**Figure S3.** (a) TEM image of PS<sub>0</sub>P2VP<sub>100</sub> (M)/Au NP. Inset shows the identification process for Au NPs by a contrast thresholding using Inspect3D software on the TEM instrument. The PS<sub>0</sub>P2VP<sub>100</sub> (M)/Au NP was prepared from photoreduced PS<sub>0</sub>P2VP<sub>100</sub> (M)/AuCl<sub>4</sub><sup>-</sup>, generated from a H<sub>2</sub>SO<sub>4</sub> solution (pH = 1) of PS<sub>0</sub>P2VP<sub>100</sub> (M) and loading with KAuCl<sub>4</sub>. The software-identified Au NPs are tracked in a tomography video (Movie S1) that was generated from tilting the sample from -70° to +70°. (b) Frames, distinguished by the angle of the tilt, from the tomography video show that some of the Au NPs do not move significantly as the sample is tilted indicating that many are located in the within the PS<sub>0</sub>P2VP<sub>100</sub> (M) particle not only on its surface. See Movie S1 of the Supporting Information.

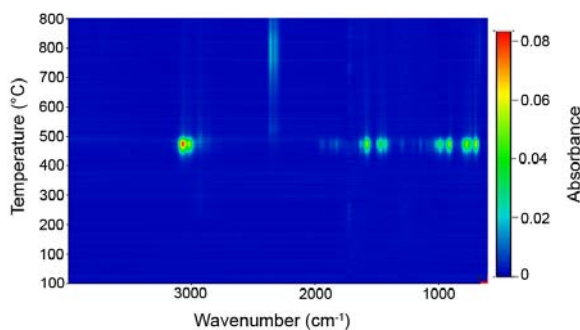
(a)



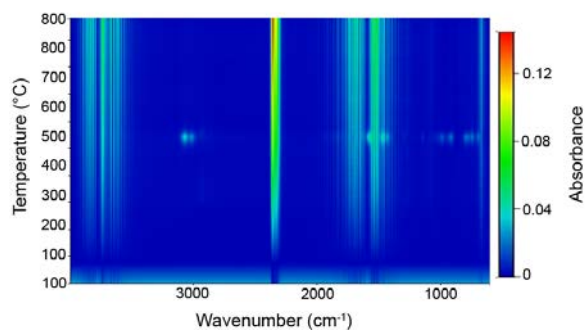
(b)



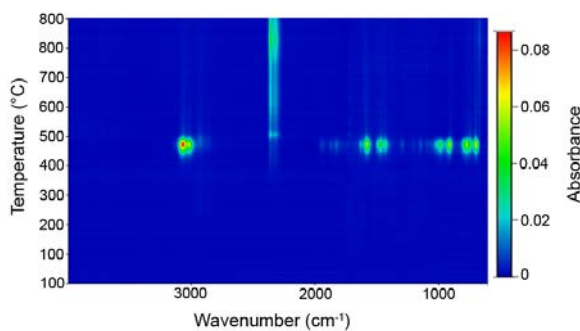
(c)



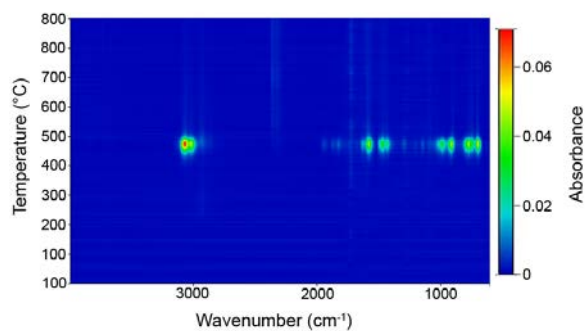
(d)



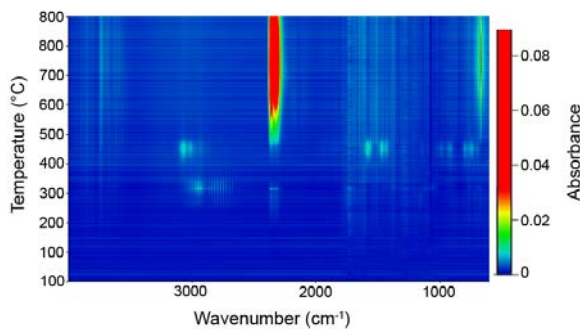
(e)



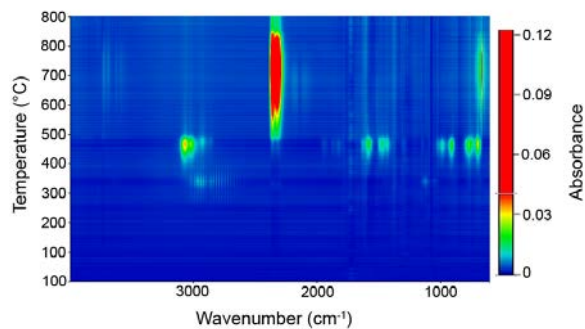
(f)



(g)



(h)



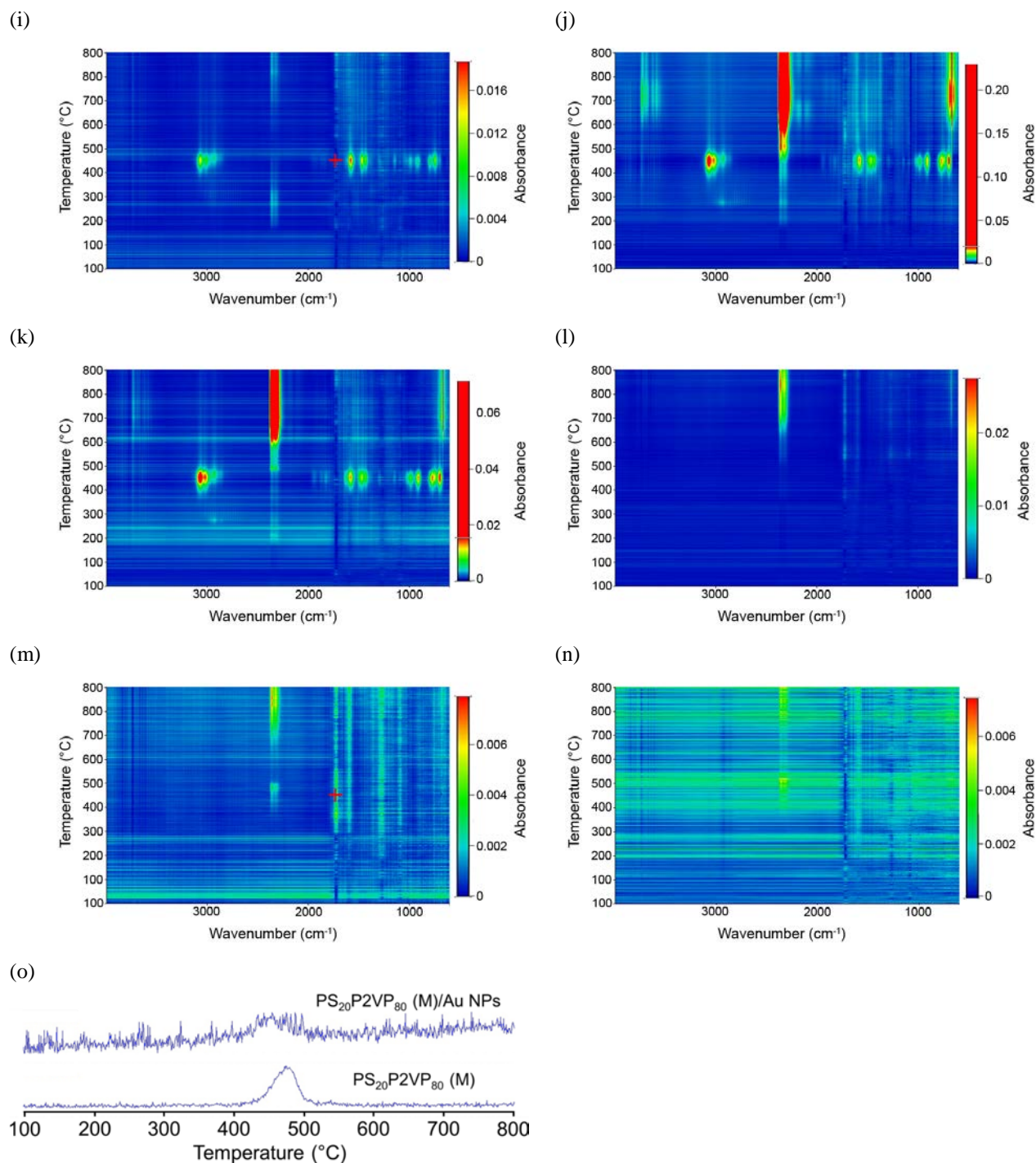


**Figure S4.** TGA-FTIR absorbance maps of (a) PS<sub>0</sub>P<sub>2VP</sub><sub>100</sub> (M), (b) PS<sub>20</sub>P<sub>2VP</sub><sub>80</sub> (M), (c) PS<sub>40</sub>P<sub>2VP</sub><sub>60</sub> (M), (d) PS<sub>60</sub>P<sub>2VP</sub><sub>40</sub> (M), (e) PS<sub>40</sub>P<sub>2VP</sub><sub>60</sub> (M) treated to the photoreduction condition, (f) PS<sub>20</sub>P<sub>2VP</sub><sub>80</sub> (M) / AuCl<sub>4</sub><sup>-</sup>, (g) PS<sub>40</sub>P<sub>2VP</sub><sub>60</sub> (M)/AuCl<sub>4</sub><sup>-</sup>, (h) PS<sub>60</sub>P<sub>2VP</sub><sub>40</sub> (M)/AuCl<sub>4</sub><sup>-</sup>, (i) PS<sub>20</sub>P<sub>2VP</sub><sub>80</sub> (M)/Au NPs, (j) PS<sub>40</sub>P<sub>2VP</sub><sub>60</sub> (M)/Au NPs, (k) PS<sub>60</sub>P<sub>2VP</sub><sub>40</sub> (M)/Au NPs, (l) PS<sub>0</sub>P<sub>2VP</sub><sub>100</sub> (M)/Ag NPs, (m) PS<sub>20</sub>P<sub>2VP</sub><sub>80</sub> (M)/Ag NPs, and (n) PS<sub>40</sub>P<sub>2VP</sub><sub>60</sub> (M)/Ag NPs. (o) FTIR tracer plots for  $\nu_{\text{benz}}$  stretch at 1635 cm<sup>-1</sup> from the effluent of PS<sub>20</sub>P<sub>2VP</sub><sub>80</sub> (M)/Au NPs and PS<sub>20</sub>P<sub>2VP</sub><sub>80</sub> (M) from TGA sample zone. For (a-n), the absorbance scale is shown as a colored intensity bar beside each map.

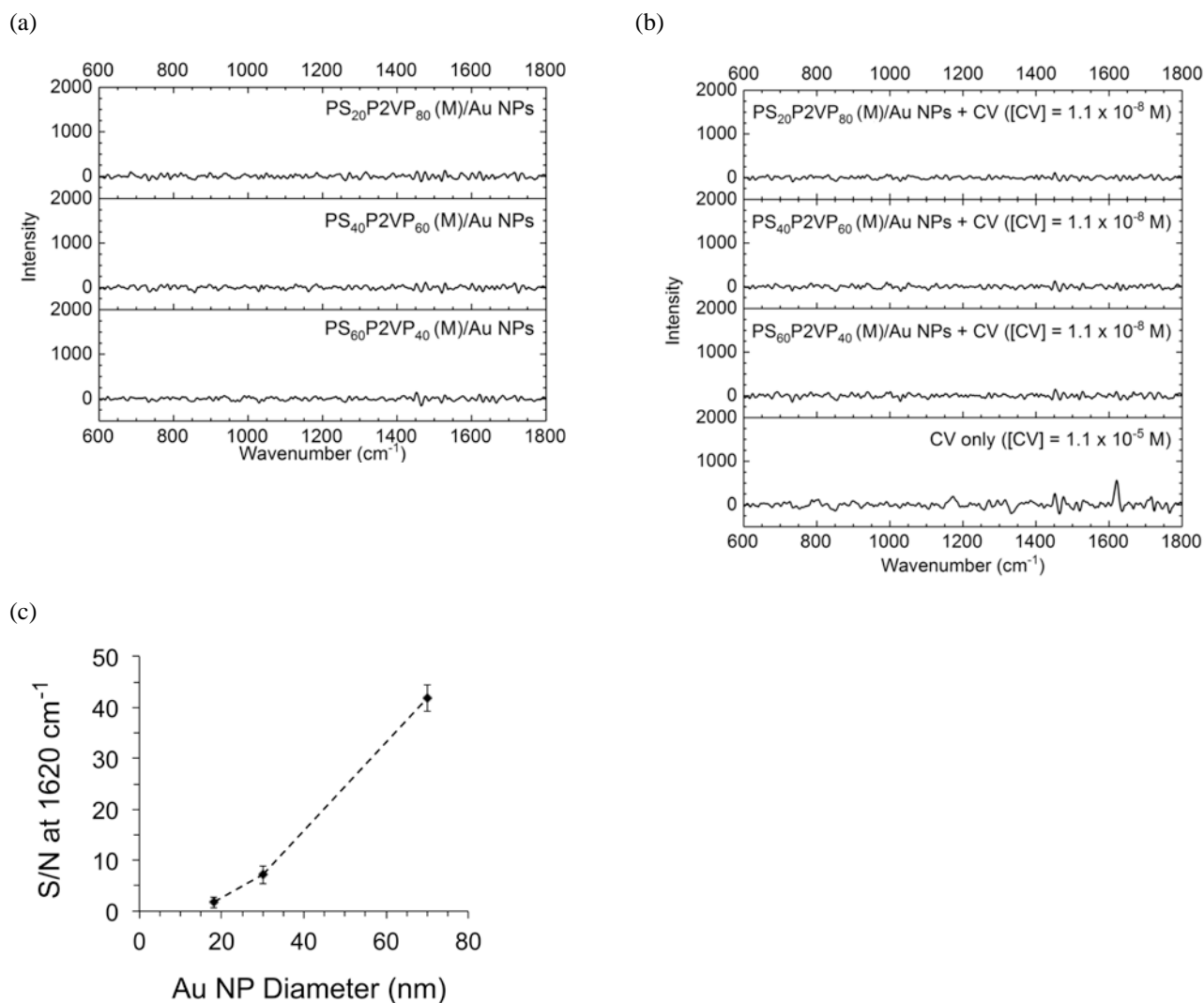


**Figure S5.** (a) Raman spectra of the PS<sub>x</sub>P2VP<sub>y</sub>(M)/Au NPs showing no signal for vibrational modes in the polymer microgel. (b) Raman spectra of the PS<sub>x</sub>P2VP<sub>y</sub>(M)/Au NPs exposed to solution-state crystal violet (CV) (concentrations indicated in legends) showing no signal for vibrational modes in the polymer microgel or the CV molecule. In (b), the Raman spectra of solution-state CV is shown at bottom for comparison. (c) S/N of the 1620 cm<sup>-1</sup> signal for CV ([CV] = 1.0 × 10<sup>-8</sup> M) versus the diameter of free Au NPs (in each case the [Au NPs] = 2.5 × 10<sup>-11</sup> M) The Au NPs were synthesized and purified according to a literature procedure.<sup>1</sup>

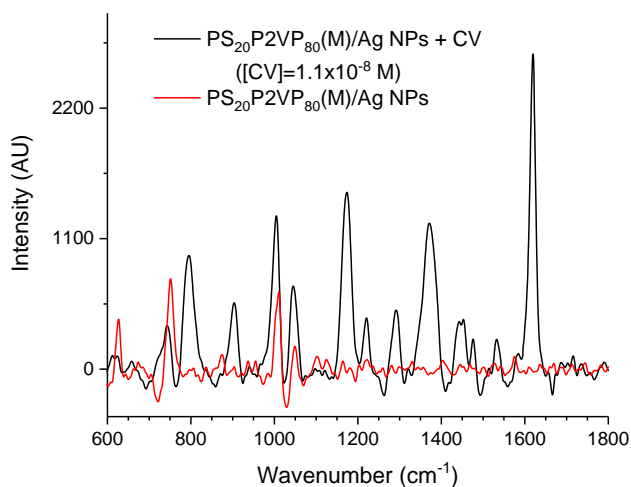


**Figure S6.** Overlay plot for the Raman spectra of the PS<sub>20</sub>P2VP<sub>80</sub> (M)/Ag NPs without (red curve) and with CV in the solution ([CV] = 1.1 x 10<sup>-8</sup> M).

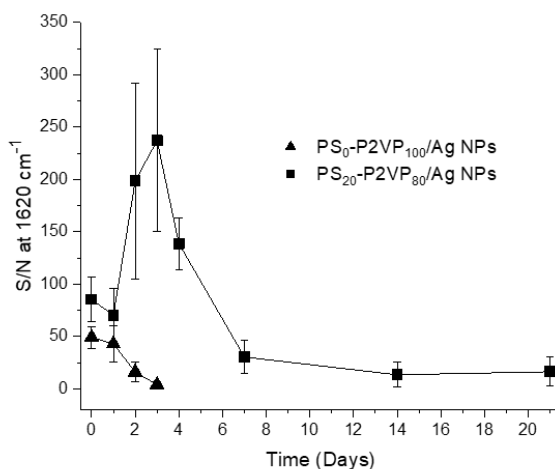


**Figure S7.** Plot for the S/N at 1620 cm<sup>-1</sup> for CV (pH = 7; [CV] = 1.1 x 10<sup>-8</sup> M) vs. time using PS<sub>20</sub>P2VP<sub>80</sub> (L)/Ag NPs (squares) and PS<sub>0</sub>P2VP<sub>100</sub> (L)/Ag NPs (triangles). On each day of the study, the pH of solutions of PS<sub>x</sub>P2VP<sub>y</sub> (L)/Ag NPs and CV was adjusted to 2 and then adjusted back to a pH value of 7, at which point the SERS spectra of CV was reacquired. The first data point (time = 0 days) therefore represents a condition that matches that for n = 1 from Figure 6d.

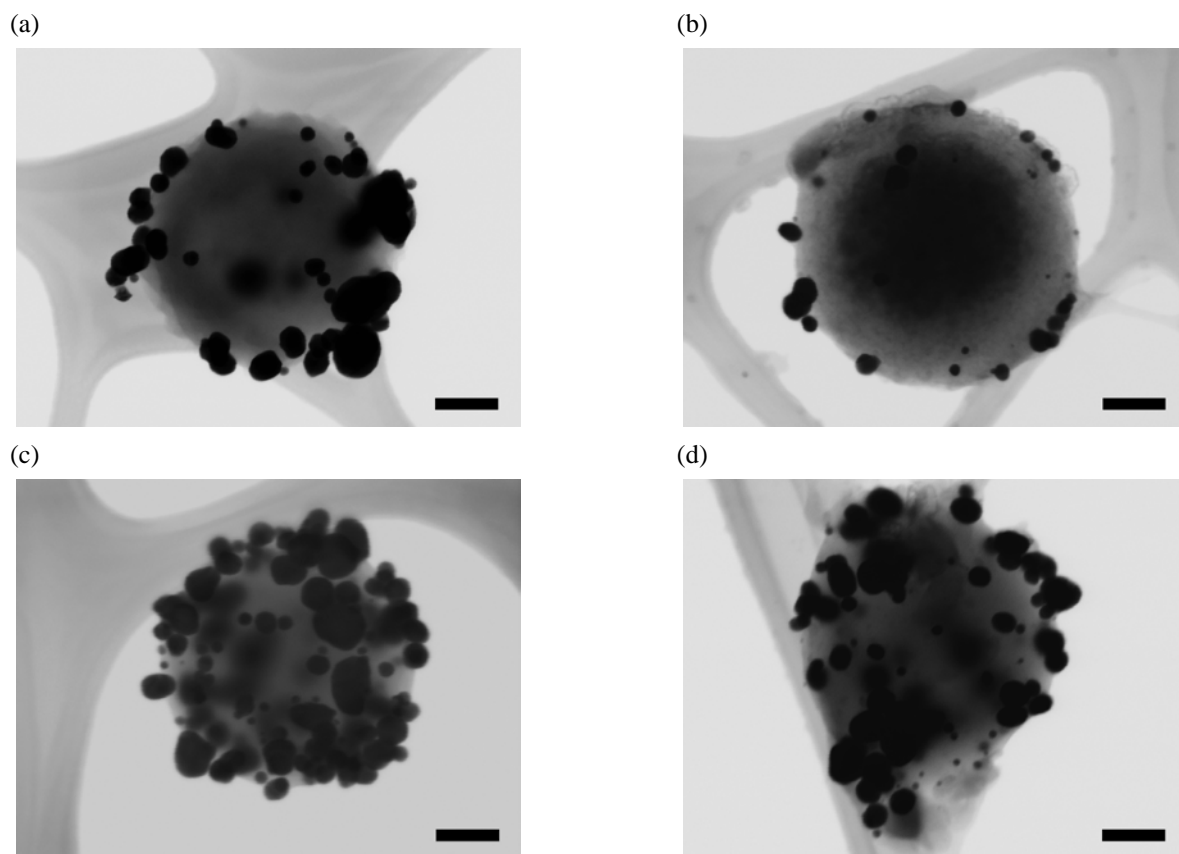
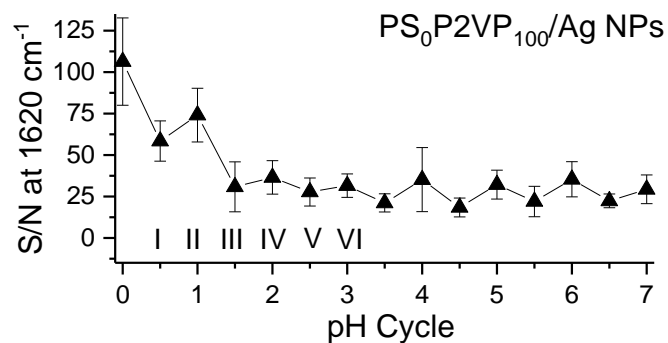


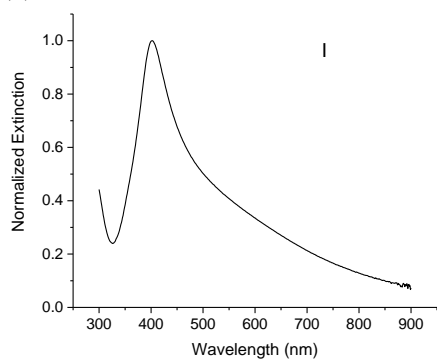
**Figure S8.** STEM images of PS<sub>0</sub>P2VP<sub>100</sub>/Ag NPs (L) after 0 pH cycles (a) and after 3 pH cycles (b). STEM image of PS<sub>20</sub>P2VP<sub>80</sub>/Ag NPs (L) after 0 pH cycles (c) and after 3 pH cycles (d). A lacey carbon support is present in all images (web-like substrate). Scale bars represent 100 nm.



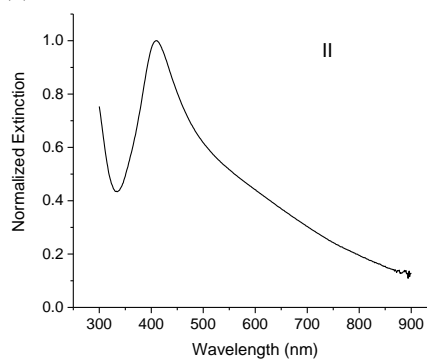
(a)



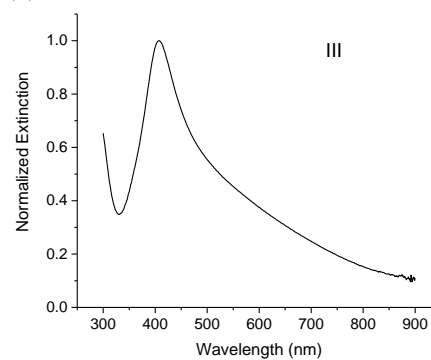
(b)



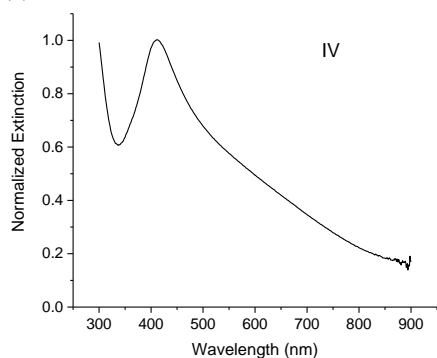
(c)



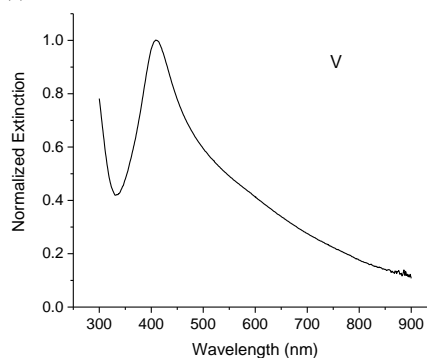
(d)



(e)



(f)



(g)

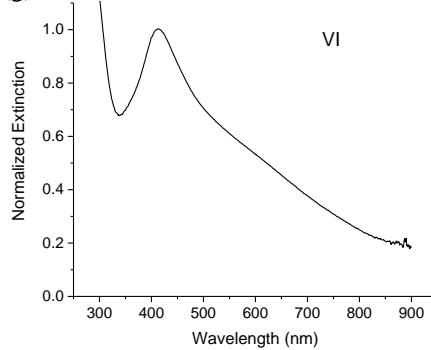
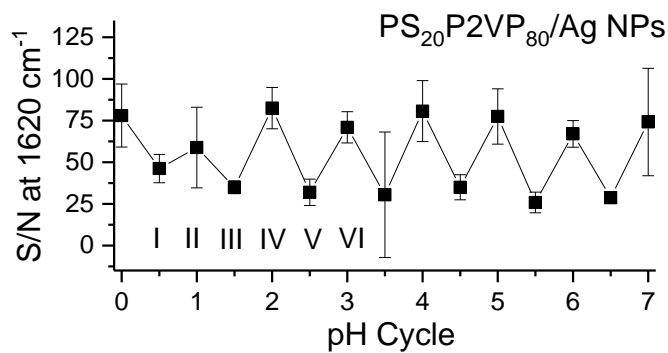
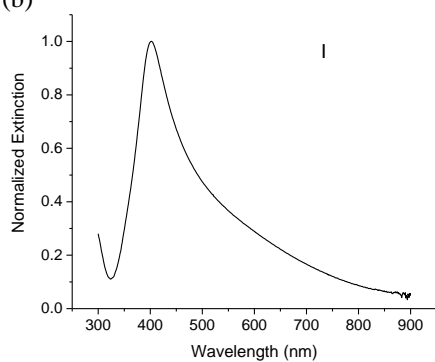


**Figure S9.** (a) Tracking of S/N of the 1620 cm<sup>-1</sup> signal for CV as the PS<sub>0</sub>P<sub>2</sub>VP<sub>100</sub>/Ag NPs (original polymer solution : pH 2.5 ultrapure water/HCl = 1:50) are cycled between the latex (integer pH cycles) and the microgel (half integer pH cycles) states by adding 41 uL of 1.71 M HCl and 82 uL of 3.0 M NaOH respectively, roman numerals represent a specific condition for the sample that that was characterized by UV-Vis (b-g).

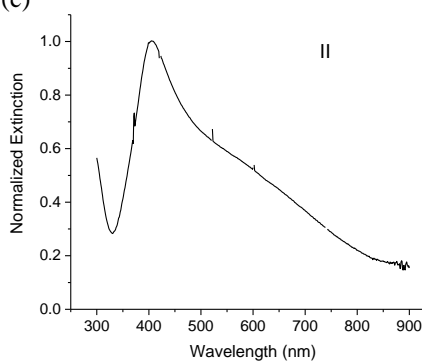
(a)



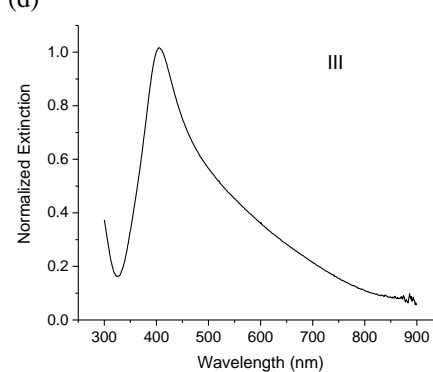
(b)



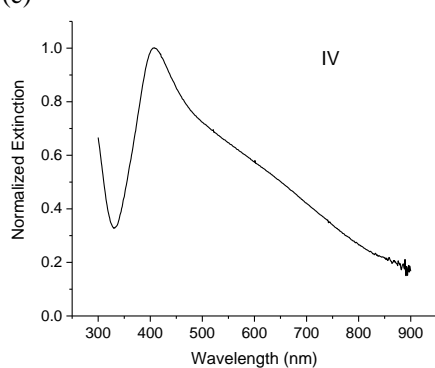
(c)



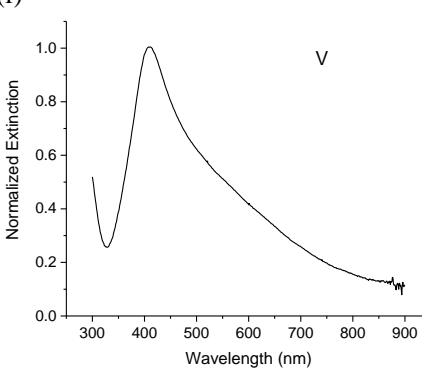
(d)



(e)



(f)



(g)

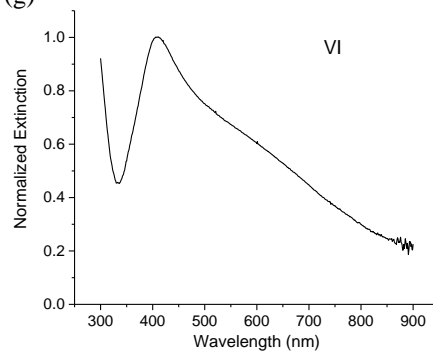


**Figure S10.** (a) Tracking of S/N of the 1620 cm<sup>-1</sup> signal for CV as the PS<sub>20</sub>P2VP<sub>80</sub>/Ag NPs (original polymer solution : pH 2.5 ultrapure water and HCl 1:50) are cycled between the latex (integer pH cycles) and the microgel (half integer pH cycles) states by adding 41 uL of 1.71 M HCl and 82 uL of 3.0 M NaOH respectively, roman numerals represent a specific condition for the sample that that was characterized by UV-Vis (b-g).

## References

- (1) Frens, G. Controlled Nucleation for the Regulation of the Particle Size in Monodisperse Gold Suspensions. *Nat. Phys. Sci.* **1973**, *241*, 20-22.